ISSN 1573-160X, *PHYSICAL OCEANOGRAPHY*, Vol. 31, Iss. 4, pp. 467-485 (2024)

published in *Morskoy Gidrofizicheskiy Zhurnal*, 2024, Vol. 40, Iss. 4, pp. 514–533

Original article

Climatic Structure and Intra-Annual Variability of Temperature Fronts on the Ocean Surface in the Patagonian Shelf Region

Yu. V. Artamonov ✉, E. A. Skripaleva, N. V. Nikolsky

Marine Hydrophysical Institute of RAS, Sevastopol, Russian Federation
✉ *artam-ant@yandex.ru*

Abstract
Purpose. The aim of the study is to analyze the features of mean long-term structure and intra-annual variability of the characteristics of temperature fronts on the ocean surface in the Patagonian shelf region.
Methods and Results. Mean daily values of the ocean surface temperature from the *NOAA OI SST* data and the geostrophic velocity components on the surface at the nodes of a 0.25° regular grid from the *CMEMS* reanalysis for 1993–2020 were used. It is shown that at the western periphery of a large-scale cyclonic meander formed by the currents in the Patagonian shelf region (south of 45°S), three branches of the Subantarctic Front are traced; they correspond to the West Falkland Current and to two jets of the East Falkland Current. North of 45°S, where one Falkland Current jet is observed, one branch of the Subantarctic Front is identified. On the eastern periphery of the meander, the front corresponding to the common stream of the Brazil Current and the Falkland Return Current is revealed. Besides, south of 40°S, a separate branch of the Subantarctic Front corresponding to one more recirculation of the Falkland Current is observed. It is shown that at the meander western periphery, the branches of the Subantarctic Front are most intensified in February – March, at its eastern periphery – in March – April, and at the meander northern peak (in the zone of the Brazil – Falkland Confluence) – in April – May and November.
Conclusions. It is found that on the western periphery of the cyclonic meander, south of 45°S, the main branch of the Subantarctic Front approximately follows the 900–1000 m isobaths, north of 45°S – the 150–170 m isobaths, and closer to the Brazil – Falkland Confluence – the 50–60 m isobaths. At the meander eastern periphery, north of 40°S, the main branch of the front is very close to the 800–1000 m isobaths, south of 40°S – to the 1000–2500 m isobaths. It has been established that the differences between the seasonal cycles of intensity of the Subantarctic Front branches are related to the dissimilar warming and cooling rates of surface waters separated by these branches.

Keywords: Patagonian shelf, large-scale cyclonic meander, bottom topography, Subantarctic Front, Falkland Current, Brazil Current, seasonal variability, horizontal temperature gradient

Acknowledgements: The study was carried out within the framework of a theme of state assignment of FSBSI FRC MHI FNNN-2024-0014 “Fundamental studies of interaction processes in the sea – air system which form variability of marine environment physical state at different spatial and temporal scales”.

For citation: Artamonov, Yu.V., Skripaleva, E.A. and Nikolsky, N.V., 2024. Climatic Structure and Intra-Annual Variability of Temperature Fronts on the Ocean Surface in the Patagonian Shelf Region. *Physical Oceanography*, 31(4), pp. 467-485.

Introduction

It is known that the flow of the Northern Branch of the Antarctic Circumpolar Current (NB ACC) when exiting the Drake Passage turns along an anticyclonic

trajectory in the area of the Birdwood Bank and penetrates to the north [1] in the form of several jets [1–11]. These jets go around the Falkland Islands in the form of the Western (WFC) and Eastern (EFC) Falkland Currents and pass over the Patagonian Shelf and the continental slope. North of 45°S, the WBC and EBC practically merge forming the common Falkland (Malvinas) Current (FC). Part of the FC flow in the area of 38–40°S turns to the south forming a large-scale cyclonic meander over the Patagonian Shelf and the continental slope. The other part of the FC flow goes north and meets the Brazil Current (BC) forming a confluence zone of these currents at approximately 36–38°S. At approximately 45°S, the eastern periphery of the cyclonic meander (Falkland Return Current, FRC) turns east and then follows the northern boundary of the Falkland Plateau as NB ACC [1] [1, 3–6, 11–17]. The northward transport of cold subantarctic waters by the Falkland Current leads to the formation of intense hydrological fronts in the Patagonian shelf region and continental slope which are zones of increased bioproductivity according to [14, 15, 18–20]. High commercial importance of the Patagonian shelf waters has led to increased interest in the variability of the frontal structure in this area. Most studies [1, 3, 4, 6, 8, 12, 14–17, 21, 22] focus on the analysis of the structure of currents or dynamic fronts. It is shown that FC is characterized by a multi-jet structure, with two most intense jets being distinguished – coastal and seaward. Their cores (velocity maxima) are located on relatively flat sections of the shelf slope where the bottom depth is approximately 150–200 and 1400–1500 m, respectively [15, 17].

Some studies have shown that there is a connection between the FC jets and the fronts in the sea surface temperature (SST) field. The maxima (in absolute value) of its negative zonal gradients coincide with the maximum meridional current velocities [14, 15]. However, studies that analyze the structural features and variability of temperature fronts in the Patagonian shelf region are relatively few in number, and the temperature fronts associated with the FC jet system have different names: the Patagonian shelf front [14], the Falkland or Malvinas front [15] and the Subantarctic Front (SAF) [2, 7, 23]. In the present paper, we will adhere to one terminology and call all temperature fronts associated with the FC jets SAF branches. Some inconsistencies in the structure and position of the SAF branches are observed in the studies of different authors based on different data. Thus, in [23], based on the World Ocean Atlas–1994 hydrological array, it is shown that the SAF position in the temperature field along the Patagonian continental slope is stable throughout the year and repeats the configuration of the 500–700 m isobaths. In [14], based on satellite SST data from the *NOAA/NASA Pathfinder* array, several temperature fronts are identified separating shelf waters from the colder waters transported by the FC, with the most intense front located near the 200 m isobath. In [15], based on contact measurements and MODIS Aqua satellite images, it is concluded that the most intense temperature SAF passes along the 1400 m isobath.

It should also be noted that the intra-annual variability of the SAF characteristics has been poorly studied: relatively short data time series analyzed insufficiently to obtain statistically reliable climate norms or front variability considered in individual sections which does not allow estimating its features along the entire length of

[1] Sarukhanyan, E.I. and Smirnov, N.P., 1986. *Water Masses and Circulation of the Southern Ocean*. Leningrad: Gidrometeoizdat, 288 p. (in Russian).

the front [7, 14]. Currently, it has become possible to use long-term data series of ocean reanalyses and arrays obtained by optimal interpolation of contact and satellite measurements with high spatio-temporal resolution to study the structure and variability of fronts. The aim of this work is to refine mean long-term spatial structure of fronts in the SST field and the climatic seasonal variability of their characteristics in the Patagonian shelf region based on the NOAA OI SST array data for 1993–2020.

Materials and methods

The paper examines the southwest Atlantic region located above the Patagonian shelf and the continental slope between the Falkland Islands and 35°S, bounded on the west by 50°W (Fig. 1, *a*). The bottom topography scheme is constructed using data from the General Bathymetric Chart of the Oceans (GEBCO) available at: http://www.gebco.net/data_and_products/gridded_bathymetry_data/ with a spatial resolution of 15 arc seconds.

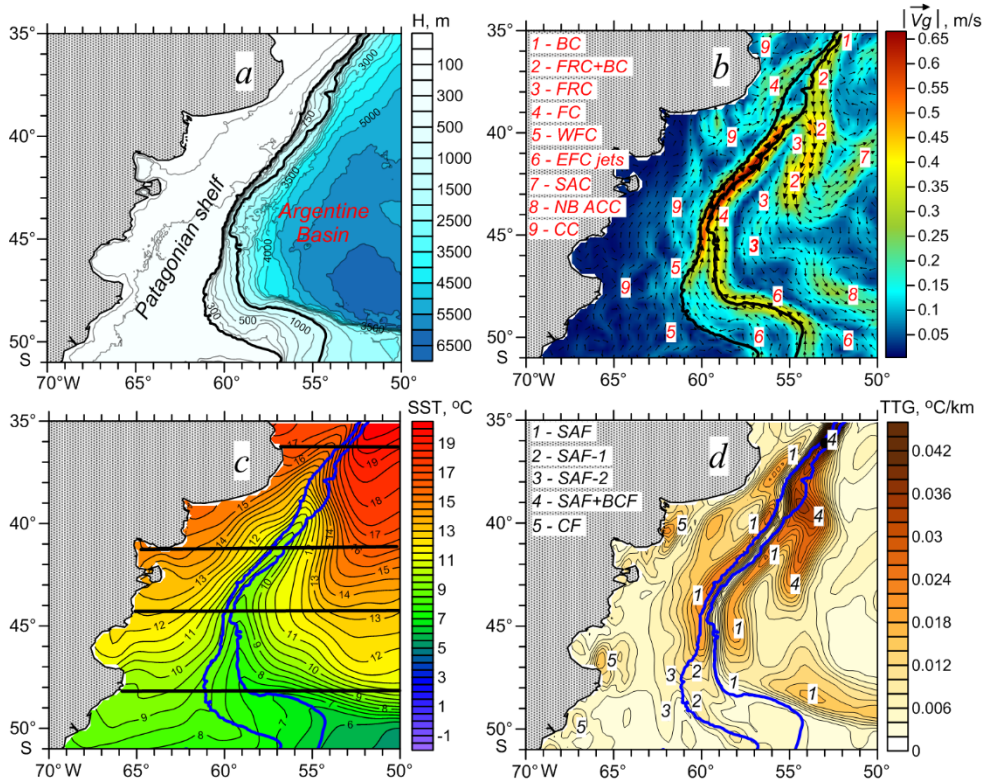

F i g. 1. Scheme of the bottom relief in the study area (*a*), spatial distribution of the mean long-term values of velocity module $|\vec{Vg}|$ and the geostrophic current vectors (*b*), temperature (SST) (*c*) and total temperature gradient (TTG) (*d*) on the sea surface. Bold lines indicate locations of the 200 m and 1400 m isobaths. Horizontal lines show the parallels for which the climatic mean annual and monthly distributions of ZTG and the meridional velocity component *Vg* are presented. Abbreviation decoding: BC – Brazil Current, FC – Falkland Current, FRC – Falkland Return Current, WFC – West Falkland Current, EFC – East Falkland Current, SAC – South Atlantic Current, NB ACC – Northern Branch of the Antarctic Circumpolar Current, CC – coastal currents, SAF – Subantarctic Front, BCF – Brazil Current Front, CF – coastal fronts

Structure and variability of temperature fronts were studied using the *NOAA Optimum Interpolation Sea Surface Temperature (OI SST)* data available at: https://www.ncei.noaa.gov/data/sea-surface-temperature-optimum-interpolation/v2.1/access/avhrr/ which contains mean daily SST values at the regular grid nodes with a step of 0.25° for 1993–2020 obtained by the method of optimal interpolation of satellite and contact measurement data [24]. The formation of temperature fronts on the surface is associated with water circulation (with advection of cold and warm waters by oppositely directed currents). Therefore, to interpret the spatial structure features of fronts in the SST field, the mean long-term structure of currents obtained based on the *Copernicus Marine Environment Monitoring Service (CMEMS)* reanalysis (http://marine.copernicus.eu/?option=com_csw&view=details&product_id=SEALEVEL_GLO_PHY_L4_REP_OBSERVATIONS_008_047) was analyzed. The reanalysis data represent mean daily values of geostrophic velocity components on the surface at the regular grid nodes with a step of 0.25° for 1993–2020. It should be noted that the reanalyses included in *CMEMS* are in good agreement with *in situ* measurements in the Patagonian shelf region [17]. In [22], high consistency of geostrophic velocities on the surface with actual velocity measurements is also noted.

The geostrophic velocities from the array used in the present paper were compared with the total velocities, including the wind drift component, according to the *ECMWF ORAS*5 and *GLORYS*2*V*4 reanalyses included in *CMEMS*. It was found that the positions of the main maxima of the geostrophic and total velocities practically coincided. Minor differences in the velocity values between the total and geostrophic currents are insignificant for solving our problem since we consider the mean long-term structure of currents and the position of flows only for interpreting the spatial structure of temperature fronts.

The same grid step of the initial data arrays and the coincidence of the coordinates of its nodes permits to compare the position of the cores of geostrophic currents and temperature fronts correctly and the time period of the 28-year data is sufficient to obtain statistically reliable mean SST and geostrophic velocity characteristics [2].

Based on the initial mean daily SST values and the geostrophic velocity components, their climatic mean monthly and long-term values were calculated at each grid node and then used to calculate meridional, zonal and full horizontal SST gradients, velocity module $|\vec{Vg}|$ and current vectors direction.

In the region under consideration, temperature fronts and currents have mainly a quasi-meridional orientation, therefore, when identifying fronts in the SST field, the criterion of the maximum (in absolute value) of the zonal temperature gradient (ZTG) was used, and when identifying the current core, the criterion of the maximum of the meridional component of the geostrophic velocity *Vg* was used. A positive or negative value of the ZTG shows an increase or decrease in temperature in the direction from west to east. The front intensity is understood as

[2] Monin, A.S., 1999. *Hydrodynamics of the Atmosphere, Ocean and Earth's Interior*. Saint Petersburg: Gidrometeoizdat, 524 p. (in Russian).

the value of the maximum of the gradient corresponding to the front. The position of temperature fronts and current cores was determined on the ZTG and *Vg* samples along parallels with a step of 0.25° at latitude.

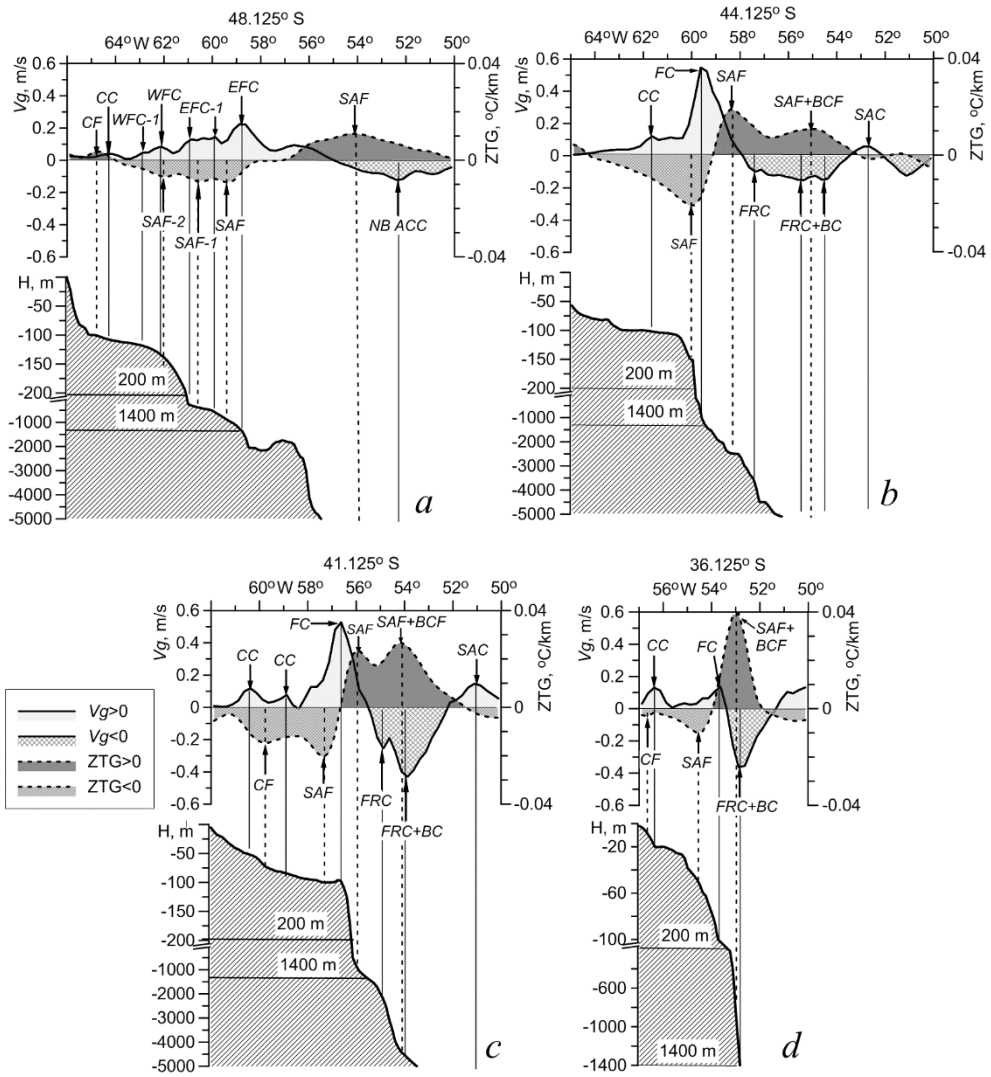

F i g. 2. Distributions of mean long-term values of ZTG (dashed curves) and *Vg* (solid curves) along 48.125°S (*a*), 44.125°S (*b*), 41.125°S (*c*) and 36.125°S (*d*) against the background of bottom profile (shaded). Positions of temperature fronts are shown by dashed lines, and those of current jets – by solid ones

Research results

Spatial distributions of the mean annual values of geostrophic velocity module and vectors (Fig. 1, *b*) show that the position of the current jets in the Patagonian shelf region is largely determined by the bottom topography features (Fig. 1, *a*). Note that coastal currents are traced over the shallowest part of the shelf with depths < 50–100 m and they are not associated with the large-scale cyclonic

meander formed by the Falkland Current (Figs. 1, *b*; 2). In the southern part of the study area (south of 45°S), where the shelf widens and relatively flat areas of the continental slope (terraces) are observed (Fig. 1, *a*), the West and East Falkland Currents are characterized by a multi-jet structure. Over the shelf with depths of 100–150 m, two weak West Falkland Current (WFC and WFC-1) jets can be observed. Seaward, between the 200 and 500 m isobaths, a wide flow corresponding to a relatively weak jet of the East Falkland Current (EFC-1) is observed. The most intense EFC jet passes over the continental slope approximately along the 1400 m isobath (Figs. 1, *b*; 2, *a*). The position of the main EFC jet in the mean long-term field of geostrophic velocity is in good agreement with the data of actual measurements carried out in this region in different years [15, 21]. Another weak EFC jet passes in the southern part of the Argentine Basin, approximately along the 2400–2500 m isobaths (Fig. 1, *b*).

North of 45°S, where the 200 and 1400 m isobaths are located close to each other (Fig. 1, *a*), the WFC and EFC jets merge forming one intense FC flow which represents the western periphery of the cyclonic meander (Figs. 1, *b*; 2, *b*).

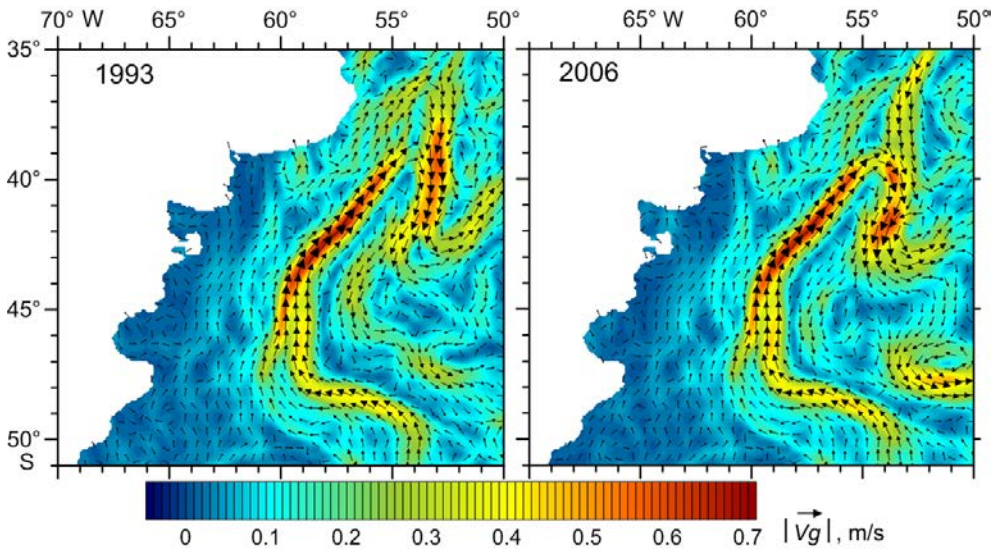

F i g. 3. Spatial distributions of the mean annual values of velocity module $|\vec{Vg}|$ and vectors of geostrophic currents for different years

In the northern part of the meander, two FC recirculation zones were identified due to the bottom topography influence. It clarifies earlier studies that identified only one FC recirculation zone [1, 3–6, 11–17]. The first zone is located at approximately 40°S, north of which a terrace between the 200 and 1400 m isobaths is observed (Fig. 1, *a*). Here, part of the FC flow turns south in the form of a FRC which passes over the continental slope approximately along the 2000–3500 m isobaths (Figs. 1, *b*; 2, *b*; 2, *c*). South of 47°S, the FRC turns east and follows the northern boundary of the Falkland Plateau as the NB ACC (Figs. 1, *b*; 2, *a*). Another part of the FC flow continues to follow north along the western edge of the terrace above the 100–200 m isobaths; it meets the Brazil Current at 35–36°S

and forms the second recirculation zone. Confluence of the BC and the FRC forms an intense common flow (FRC+BC) which follows south over the continental slope seaward of the 1400 m isobath to approximately 39°S (Figs. 1, *b*; 2, *d*). Further south, in the region of 40–41°S, part of the FRC+BC flow turns to the east and passes over the deep-water part of the Argentine Basin approximately above the 5500 m isobath. The main part of the FRC+BC flow continues to follow to the south above the 4500 m isobath (Figs. 1, *b*; 2, *c*) and between 43° and 44.5°S turns to the northeast along an anticyclonic trajectory and then follows in an easterly direction in the form of the South Atlantic Current (SAC) (Figs. 1, *b*; 2, *b*, 2, *c*).

Main circulation features revealed in the mean long-term field of geostrophic velocity are clearly seen in the distributions of current vectors and velocity module for each year (Fig. 3). Despite the interannual variability of flow intensity, the position of the main WFC, EFC, FC jets, the FRC+BC flow and two FC recirculations (in the region of 40°S and between 35° and 36°S) controlled by the bottom topography features is maintained throughout each year.

Multidirectional geostrophic flows lead to the formation of well-defined tongues of cold and warm waters in the SST field (Fig. 1, *c*), at the boundaries of which zones of increased total horizontal temperature gradients (TTG) or frontal zones (Fig. 1, *d*) are formed. According to [8, 19, 20], jets of intense currents are barriers that impede horizontal water exchange and separate water masses with different transformation degrees.

Let us present the main features of the mean long-term structure of temperature fronts formed on the peripheries of a large-scale cyclonic meander. It should be noted that over the shallow part of the shelf with depths of < 100 m, relatively weak extremes of SST gradients of different signs associated with the advection of shelf waters by coastal currents and called conventionally coastal fronts are observed (Figs. 1, *d*; 2). Since the CF branches do not belong to the system of large-scale cyclonic meander fronts, they are not discussed in this paper.

On the southwestern periphery of the meander south of 45°S, three fronts are identified as the SAF branches. The eastern branch (the SAF itself), most intense of them, passes approximately 0.5° west of the main EFC jet above the 900–1000 m isobaths. The weaker central branch (SAF-1) is located within the EFC-1 flow above the 300–400 m isobaths. The western branch (SAF-2) coincides practically with the WFC jet and is observed above the 130–150 m isobaths (Fig. 2, *a*). North of 45°S, where the western periphery of the meander is formed by a single FC flow, the SAF is also represented by a single branch. Here, the front is located approximately 0.25° west of the FC flow above the 150–170 m isobaths (Fig. 2, *b*). In the northwestern part of the meander, the SAF passes above the 100 m isobath, while its position shift to the west relative to the FC core position increases gradually and at the 41°S latitude reaches 0.5° (Fig. 2, *c*). Closer to the Brazil – Falkland Confluence, the SAF is located above depths of 50–60 m, noticeably weakens and shifts to the west relative to the FC by almost 1° (Fig. 2, *d*). On the north-eastern periphery of the cyclonic meander formed by the common FRC+BC flow, an intense

front is observed in the SST field. It is formed as a result of the convergence of the Subantarctic Front and the Brazil Current Front (SAF+BCF). This front passes over the 800–1000 m isobaths and coincides practically in position with the core of RB FC+BC (Fig. 2, *d*). Up to approximately 39–40°S, the SAF+BCF separates the cold waters transported by the FC and the warm waters transported by the FRC+BC flow. On the eastern periphery of the meander south of 40°S, a wide zone of high ZTG values is observed. Within this zone, to the west of the main ZTG maximum corresponding to the SAF+BCF, another ZTG maximum is distinguished corresponding to another SAF branch (Fig. 2, *c*). Formation of two temperature fronts in this section of the meander is associated with two southerly flows (the FRC and the general FRC+BC flow). Here, the SAF separates the coldest waters transported by FC from the south from warmer waters coming from the north with the FRC and the SAF+BCF, in turn, separates the latter from even warmer waters transported by the FRC+BC. The SAF+BCF branch coincides practically in position with the FRC+BC core and the SAF is shifted to the west of the FRC jet by almost 1° (Fig. 2, *c*). These two fronts (SAF and SAF+BCF) persist up to approximately 45°S, with the SAF being observed over the continental slope along the 1000–2500 m isobaths and gradually strengthening in the southern direction while the SAF+BCF passes over depths greater than 4000 m and, conversely, weakens gradually (Figs. 2, *b*; 2, *c*). It should be noted that the identification of two SAF branches on the eastern periphery of the meander between 40° and 45°S clarifies the earlier results of [14] which noted the existence of one seaward temperature front south of 40°S characterized by weak positive SST gradients.

In general, the performed analysis of the relationship between the position of the SAF branches and the bottom topography features showed that, in contrast to previously obtained results [14, 15, 23], the main SAF branch passes over different isobaths in different water area parts: in the southwestern part – over the 900–1000 m isobaths, north of 45°S – over the 150–170 m isobaths, at the top of the cyclonic meander – over the 50–60 m isobaths, on the eastern periphery of the meander up to approximately 40°S – above the 800–1000 m isobaths and to the south – above the 1000–2500 m isobaths.

It should be noted that, in general, on the large-scale meander peripheries, the temperature fronts on the surface either coincide in position with the cores of geostrophic currents or are located to the west, while the maximum shift does not exceed 1° at longitude and is noted on the eastern periphery of the meander.

South of 47–48°S, where the FRC+BC flow turns east and follows the northern boundary of the Falkland Plateau as NB ACC, the mean annual SST field exhibits one main ZTG extreme corresponding to the SAF (Fig. 2, *a*).

Analysis of the mean monthly SST distributions showed that, despite the high seasonal variability, well-defined tongues of cold and warm waters are observed throughout the year (Fig. 4), as a result of which the main features of the mean annual frontal structure are observed during all months (Fig. 5).

Distributions of the climatic mean monthly zonal SST gradients showed that the SAF branches influenced by bottom topography, especially on the western

periphery of the meander, have a stable position, with their intra-annual shifts at longitude not exceeding 1° (Figs. 5, 6). At the same time, the intra-annual changes in the intensity of the SAF branches differ significantly in various parts of the water area. Thus, their values do not exceed 0.012 °C/km in the south (Fig. 6, *a*), increase to 0.016–0.02 °C/km north of 45°S (Figs. 6, *b*; 6, *c*), decrease again at the top of the meander and are 0.006 °C/km at 35–36°S (Fig. 6, *d*). The values of seasonal changes in the SAF+BCF intensity decrease in the southerly direction from 0.04–0.05 °C/km at 35–36°S to 0.012 °C/km at 44°S (Figs. 6, *b–d*).

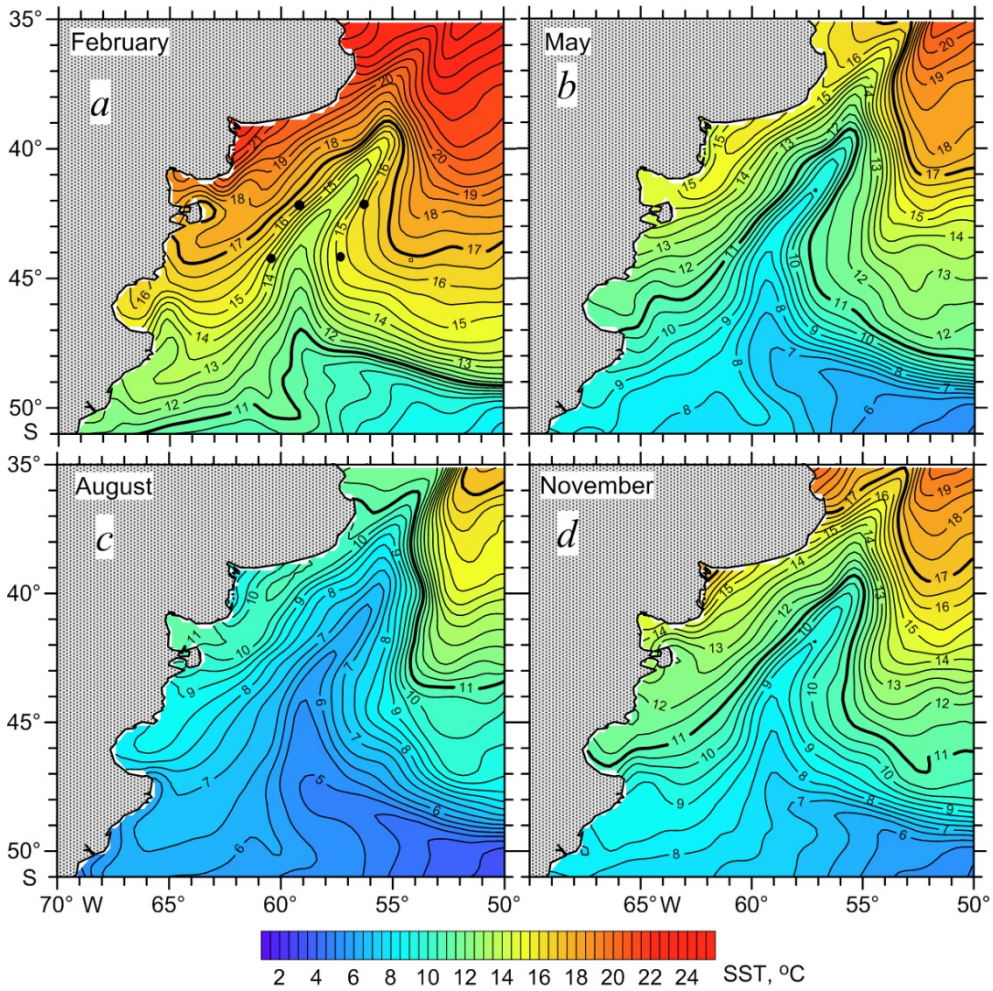

F i g. 4. Distributions of the climatic mean monthly SST values in February (*a*), May (*b*), August (*c*) and November (*d*). Bold lines denote the 11°C and 17°C isotherms

Differences in the periods of maximum intensification of fronts in different areas of the western (Fig. 7, *a*) and eastern (Fig. 7, *b*) peripheries of the large-scale meander are also noted.

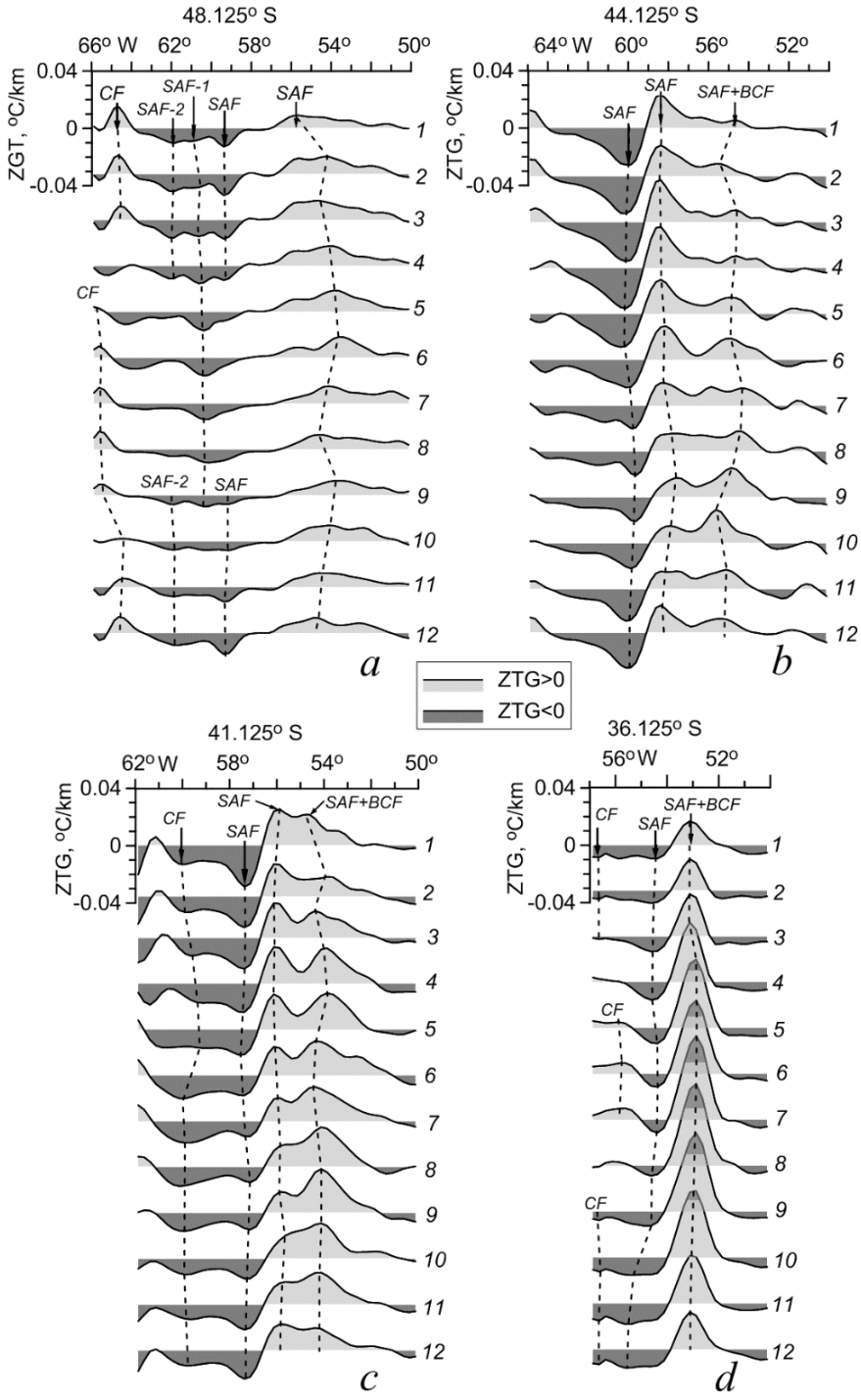

F i g. 5. Distributions of the climatic mean monthly ZTG values along 48.125°S (*a*), 44.125°S (*b*), 41.125°S (*c*) and 36.125°S (*d*). Positions of temperature fronts are shown by dashed lines, numerals by the curves are months

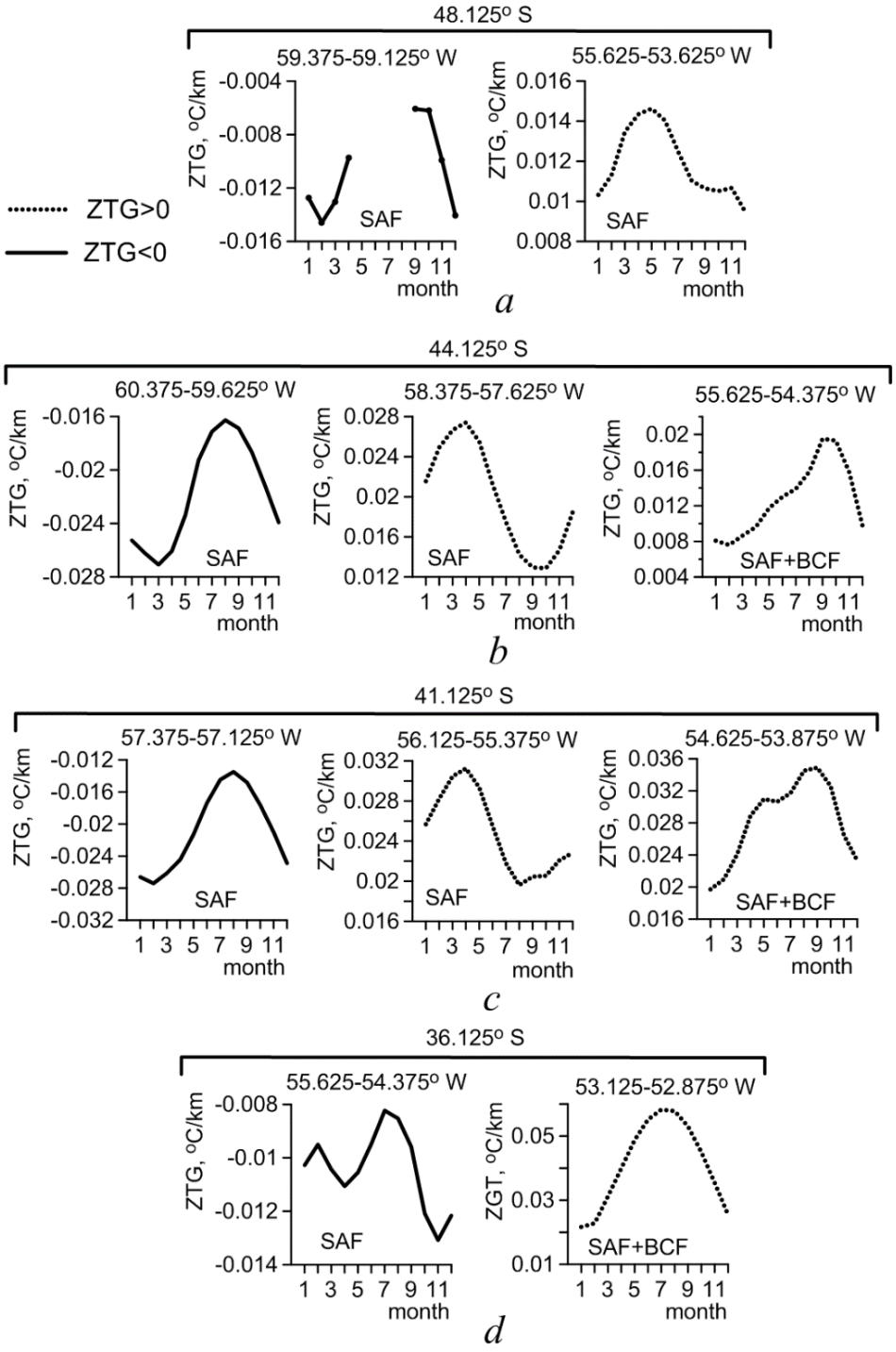

F i g. 6. Graphs of climatic seasonal cycle of SAF and SAF+BCF intensity and range of their longitudinal displacement during a year (shown on the graphs) on 48.125°S (*a*), 44.125°S (*b*), 41.125°S (*c*) and 36.125°S (*d*)

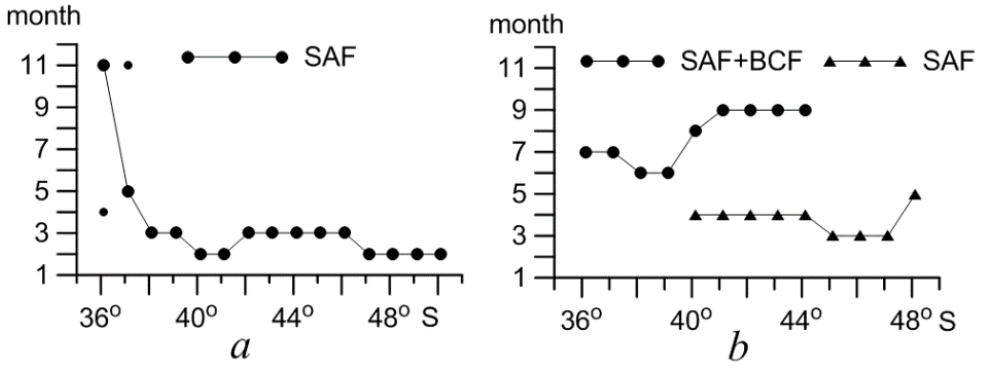

F i g. 7. Month of maximum intensification of SAF and SAF+BCF at the western (*a*) and eastern (*b*) peripheries of a cyclonic meander. Dots in fragment a show the onset of the second, weaker, maximum of SAF intensity

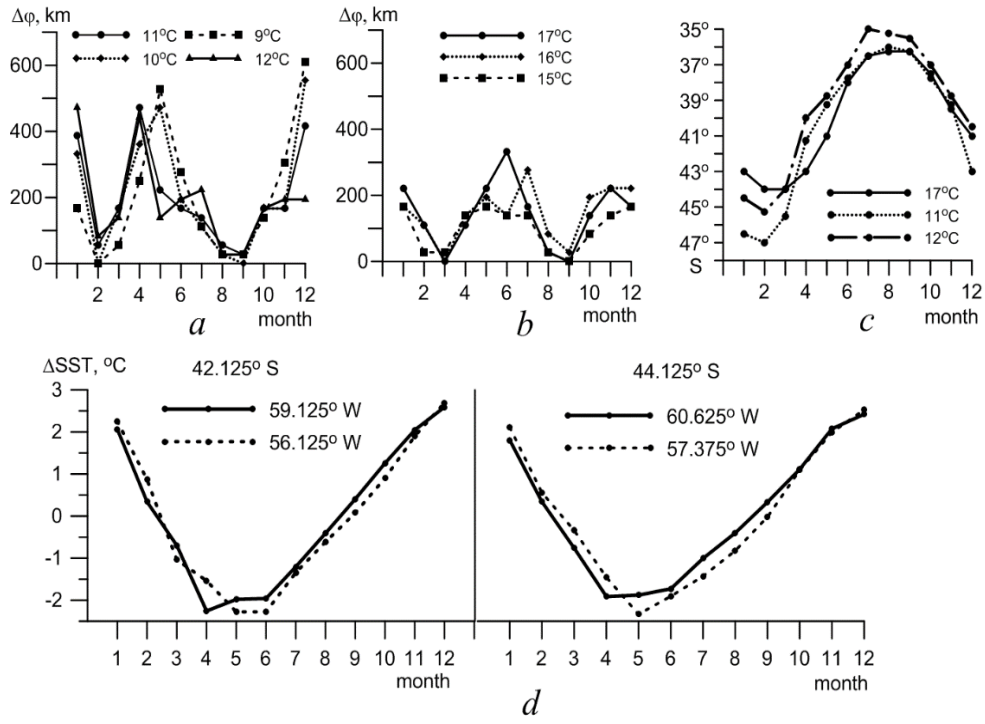

F i g. 8. Displacement (at latitude) speed (km/month) of various isotherms in the tongues of cold (*a*) and warm (*b*) waters; extreme northern position of the 11 °C and 12 °C isotherms in the cold water tongue and extreme southern position of the 17 °C isotherm in the warm water tongue for each month (*c*); ΔSST intra-annual cycle in certain grid knots (shown by points in Fig. 4, *a*) at the western (solid curves) and eastern (dotted curves) meander peripheries (*d*)

Seasonal variability features of front intensity in the SST field are associated with differences in the rate of intra-annual shifts of isotherms in the tongues of cold and warm waters (Fig. 4) caused by the combined influence of advection and seasonal warming/cooling of surface waters separated by fronts.

The paper estimates the latitude shifts during the year of the 9–12°C and 15–17°C isotherms, typical for cold and warm water tongues, respectively. For this purpose, the difference in kilometers (Δφ) between the extreme northern and extreme southern positions of these isotherms in cold and warm water tongues, respectively, in January relative to December, in February relative to January, etc. was calculated (Figs. 8, *a*; 8, *b*).

Intra-annual variations of Δφ show that during the periods of maximum warming (February – March) and cooling (August – September) of surface waters [3] these isotherms change their latitudinal position slightly. In April – May, when intensive cooling of waters takes place, the 9–12 °C isotherms shift northwards almost 450–500 km. With warming up of surface waters in October – February, they shift southwards. The maximum shifts reflecting the greatest rate of warming for the 9–11 °C isotherms are observed in December with Δφ values reaching 400–600 km; for the 12 °C isotherm – in January with Δφ values of ~ 500 km (Fig. 8, *a*). It is worth noting that the intra-annual variations of Δφ for the 15–17 °C isotherms in the warm water tongue are similar to the variations of Δφ for the 9–12 °C isotherms, but their values decrease and do not exceed 200–300 km (Fig. 8, *b*). In general, during the year, the shifts of the northern boundary of the cold water tongue according to the 11 °C and 12 °C isotherms and the southern boundary of the warm water tongue according to the 17 °C isotherm from the extreme southern to the extreme northern position reach 11°, 12°, and 8° latitudes, respectively (Fig. 8, *c*).

Note the following features analyzing the relationship between the seasonal variability of the SAF branches intensity and the isotherms shift in the cold and warm water tongues. On the southwestern periphery of the meander, the western (SAF-2) and eastern (SAF) branches of the Subantarctic Front are most clearly observed during the warm season of the Southern Hemisphere (Fig. 5, *a*). During this period, SAF-2 separates the warmed shelf waters from the colder waters carried by the WFC and the SAF separates the waters carried by the EFC-1 flow from even colder waters carried by the main branch of the EFC (Fig. 4, *a*). These fronts become most intense in February – March (Figs. 6, *a*; 7, *a*) when the maximum warming of the waters in the southern part of the shelf is observed (SST values > 12.5–13 °C) (Fig. 4, *a*). During these months, the northern boundary of the cold water tongue along the 9–12 °C isotherms is located in the south and only changes its latitudinal

[3] Lomakin, P.D. and Skripaleva, E.A., 2008. *The Circulation and Water Structure in the Southwest Atlantic and Antarctic Adjacent Areas*. Sevastopol: EKOSI-Gydrofizica, 116 p. (in Russian).

position slightly (Figs. 8, *a*; 8, *c*). During the cold season (from May to August), the SST values over the southern part of the shelf do not exceed 7–9 °C (Figs. 4, *b*; 4, *c*). Temperature contrasts between the coastal waters and the waters carried by the WFC and EFC decrease noticeably, which leads to SAF-2 and SAF weakening (Fig. 6, *a*). During this period, the EFC-1 flow brings colder waters with temperatures < 6–8 °C from the south (Figs. 4, *b*; 4, *c*). Judging by the rapid shift of the 9–10°C isotherms to the north, it can be noted that the maximum decrease rate of SST values in the cold water tongue is observed in May (Fig. 8, *a*). This leads to an increase in temperature contrasts in the zone of the SAF-1 front central branch, the greatest intensification of which is observed in May – June (Fig. 5, *a*).

North of 45°S, the SAF structure exhibits one branch throughout the year which is the western boundary of the tongue of cold waters transported by the FC separating them from the warmer shelf waters (Figs. 5, *b* – *d*). Here, the maximum SAF intensification occurs in February – March (Figs. 6, *b*, *c*; 7, *a*) when the maximum warming of surface waters is observed. During this period, the 9–12 °C isotherms in the tongue of cold waters do not practically change their latitudinal position and are maximally shifted to the south (Figs. 8, *a*, *c*). The intensification of temperature contrasts supporting the front is due to more intense warming of the shelf waters where the SST values increase in the northerly direction from 16 °C to 21°C during this period, while they change from 12 °C to 17 °C to the east of the front in the tongue of cold waters (Fig. 4, *a*).

So, the main branch of the SAF intensifies in February – March on the entire western periphery of the meander, whereas a longer period of front intensification from November to May in [14] and from December to March in [7] was noted earlier.

At the northern meander apex, in the convergence zone of the Falkland and Brazil currents which, according to [13, 25], intensify in antiphase in the Southern Hemisphere winter and summer, respectively, the SAF intensity also changes with a semi-annual period with maxima in April – May and November (Figs. 6, *d*; 7, *a*). In April – May, the SAF intensification occurs during an intense cooling period when the boundary of the cold water tongue along the 9–12 °C isotherms shifts quickly north (Figs. 8, *a*, *c*) and the temperature of the shelf waters remains quite high and exceeds 15 °C (Fig. 4, *b*). The second maximum of the SAF intensity (in November) is observed during intense warming period when the 9–12 °C isotherms in the cold water tongue shift quickly to the south (Figs. 8, *a*, *c*) and the temperature of the coastal shelf waters rises to 17–18 °C (Fig. 4, *d*).

South of the Brazil – Falkland Confluence up to approximately 40°S, where the SAF+BCF front is the boundary between the cold and warm waters carried by these currents, it intensifies in June – July when the 11–12 °C isotherms in the tongue of cold waters are shifted maximally to the north (Figs. 6, *d*; 7, *a*; 8, *a*, *c*). South of 40°S, where the SAF+BCF serves as the western boundary of the warm water tongue separating them from the colder waters carried by the FRC, it intensifies in August – September (Figs. 6, *b*, *c*; 7, *b*). During this period, maximum cooling of surface waters is observed and the 15–17 °C isotherms in the tongue of

warm waters are shifted maximally to the north (Figs. 8, *b*, *c*). Front strengthening is due to the fact that in August – September the temperature of the waters carried by the FRC does not exceed 9–10 °C while the SST values in the tongue of warm waters, despite the general cooling, remain higher and amount to 11–15 °C (Fig. 4, *c*). The Subantarctic Front which is located west of the SAF+BCF and separates the waters carried from the north by the FRC from even colder waters carried from the south by the FC intensifies in March – April (Figs. 6, *b*, *c*; 7, *b*). During this period, cooling of surface waters begins, especially pronounced in the cold tongue. According to the isotherms of 9–12 °C, its boundary shifts to the north by almost 500 km in April (Figs. 8, *a*, *c*) while the waters coming from the north with the FRC are still noticeably warmer at this time (SST values > 13–15 °C). Note that the SAF intensifies on the eastern periphery of the meander approximately a month later than on the western one (Fig. 7). According to an earlier work [7], at the eastern boundary of the cyclonic meander south of 42°S, the SAF intensified in May – June, i.e. the delay in the onset of the maximum compared to the western periphery was almost half a year. Analysis of the intra-annual course of the temperature change rate ΔSST (difference between the SST values of the current and previous months) showed that a similar phase delay of one month was observed at the onset of the maximum rate of water cooling west and east of the SAF at the western and eastern peripheries of the meander, respectively (Fig. 8, *d*). The maximum rate of water cooling (ΔSST ~ −2.5 °C) at the western periphery of the meander is observed in April, at the eastern periphery – a month later, in May.

To the south of 48°S, above the northern boundary of the Falkland Plateau, the main extremum of the ZTG in the SAF structure observed throughout the year (Fig. 5, *a*) is maximally intensified in May (Figs. 6, *a*; 7, *b*) during the period of intense cooling of surface waters.

Conclusion

Based on *NOAA OI SST* data, the spatial structure of the Subantarctic Front in the climatic field of sea surface temperature in the Patagonian shelf region has been refined and its relationship with the bottom topography features and geostrophic currents that form a large-scale cyclonic meander in this region has been analyzed.

High spatial resolution of the used data array allowed identifying several branches in the SAF structure in the mean long-term SST climatic field. For the first time, the isobaths in the SST climatic field are shown, over which these SAF branches pass in different parts of the water area. Three branches of the Subantarctic Front were identified on the western periphery of the meander south of 45°S. The main SAF branch (eastern) corresponds to the most intense EFC jet and passes over the 900–1000 m isobaths. The central and western SAF branches correspond to the weaker EFC-1 and WFC jets and pass over the 300–400 m and 130–150 m isobaths, respectively. One branch of the SAF can be observed north of 45°S. It corresponds to the FC which passes above the 150–170 m isobaths. At the top of

the cyclonic meander, closer to the Brazil – Falkland Confluence, the SAF passes above the 50–60 m isobaths.

For the first time it is shown that two FC recirculation zones leading to the formation of two SAF branches on the eastern periphery of the meander are observed as a result of topographic features (the presence of a terrace between the 200 and 1400 m isobaths north of 40°S). One branch (SAF+BCF) is formed as a result of the BC and the FRC convergence, the second one (SAF) is formed south of 40°S and corresponds to one more recirculation of the Falkland Current. These two branches can be traced to approximately 45°S. The SAF+BCF branch passes above the 800–1000 m isobaths up to 40°S, further south – above depths of > 4000 m and weakens gradually in the southern direction. The SAF is observed over the continental slope along the 1000–2500 m isobaths and intensifies gradually in the southern direction.

For the first time, the characteristics of the climatic seasonal cycle of each SAF branch on the western and eastern peripheries of the meander were obtained. It is found that the SAF branches have a stable position under the bottom topography influence, especially on the western periphery of the meander, with their intra-annual shifts not exceeding 1° at longitude. It is revealed that the values of intra-annual changes in the intensity of the SAF branches differ significantly in different parts of the water area. They do not exceed 0.012 °C/km in the south, increase to 0.016–0.02 °C/km north of 45°S, decrease again at the top of the meander and are 0.006 °C/km at 35–36°S. Seasonal changes in the SAF+BCF intensity weaken in the southern direction from 0.04–0.05 °C/km at 35–36°S up to 0.012 °C/km at 44°S.

Differences in the periods of maximum intensification of the SAF branches in different areas of the western and eastern peripheries of a large-scale meander are revealed. It is shown that they are associated with differences in the rates of heating and cooling of the waters separated by these branches. It is found that the SAF branches intensify to the maximum on the western periphery of the meander in February – March when maximum heating of the waters is observed on the shelf. The SAF intensifies on the eastern periphery of the meander south of 40°S approximately a month later, in March – April. The same one-month delay was revealed at the onset of the maximum rate of water cooling on the western and eastern peripheries of the meander. It is found that the SAF intensity changes at the northern meander apex, in the Brazil – Falkland Confluence, with a semi-annual period with the maxima in April – May during intensive cooling of waters and in November during the intensive heating period. The SAF+BCF up to approximately 40°S intensifies on the eastern periphery of the meander, south of the Brazil – Falkland Confluence, in June – July when the maximum rate of surface waters cooling is observed and south of 40°S – in August – September when the minimum SST values are observed. The SAF intensifies to the maximum over the northern boundary of the Falkland Plateau in May, during the period of surface waters intensive cooling.

REFERENCES

1. Zyryanov, V.N. and Severov, D.N., 1979. Water Circulation in the Falkland – Patagonian Region and Its Seasonal Variability. *Oceanology*, 19(5), pp. 782-791.

2. Guretsky, V.V., 1987. Surface Thermal Fronts in the Atlantic Sector of the Southern Ocean. *Meteorologiya i Gidrologiya*, (8), pp. 81-89 (in Russian).

3. Peterson, R. and Whitworth, T., 1989. The Subantarctic and Polar Fronts in Relation to Deep Water Masses through the Southwestern Atlantic. *Journal of Geophysical Research: Oceans*, 94(C8), pp. 10817-10838. https://doi.org/10.1029/JC094iC08p10817

4. Peterson, R.G. and Stramma, L., 1991. Upper-Level Circulation in the South Atlantic Ocean. *Progress in Oceanography*, 26(1), pp. 1-73. https://doi.org/10.1016/0079-6611(91)90006-8

5. Belkin, I.M., 1993. Frontal Structure of the South Atlantic. In: N. M. Voronina, ed., 1993. *Pelagic Ecosystems of the Southern Ocean*. Moscow: Nauka, pp. 40-53 (in Russian).

6. Orsi, A.H., Whitworth, T.III and Nowlin, W.D.Jr., 1995. On the Meridional Extent and Fronts of the Antarctic Circumpolar Current. *Deep Sea Research Part I: Oceanographic Research Papers*, 42(5), pp. 641-673. https://doi.org/10.1016/0967-0637(95)00021-W

7. Artamonov, Yu.V. and Skripaleva, E.A., 2005. [Structure and Seasonal Variability of the Subantarctic Front in the Southwest Atlantic from Satellite Measurements of Ocean Surface Temperature]. *Monitoring Systems of Environment*, (8), pp. 237-239 (in Russian).

8. Sokolov, S. and Rintoul, S.R., 2009. Circumpolar Structure and Distribution of the Antarctic Circumpolar Current Fronts: 1. Mean Circumpolar Paths. *Journal of Geophysical Research: Oceans*, 114(C11), C11018. https://doi.org/10.1029/2008JC005108

9. Barré, N., Provost, C., Renault, A. and Sennéchael, N., 2011. Fronts, Meanders and Eddies in Drake Passage during the ANT-XXIII/3 Cruise in January–February 2006: A Satellite Perspective. *Deep Sea Research Part II: Topical Studies in Oceanography*, 58(25-26), pp. 2533-2554. https://doi.org/10.1016/j.dsr2.2011.01.003

10. Graham, R.M., de Boer, A.M., Heywood, K.J. and Chapman, M.R., 2012. Southern Ocean Fronts: Controlled by Wind or Topography? *Journal of Geophysical Research: Oceans*, 117(C8), C08018. https://doi.org/10.1029/2012JC007887

11. Artamonov, Yu.V., Skripaleva, E.A. and Nikolsky, N.V., 2022. Climatic Structure of the Dynamic and Temperature Fronts in the Scotia Sea and the Adjacent Water Areas. *Physical Oceanography*, 29(2), pp. 117-138. https://doi.org/10.22449/1573-160X-2022-2-117-138

12. Roden, G.I., 1986. Thermohaline Fronts and Baroclinic Flow in the Argentine Basin during the Austral Spring of 1984. *Journal of Geophysical Research: Oceans*, 91(C4), pp. 5075-5093. https://doi.org/10.1029/JC091iC04p05075

13. Remeslo, A.V., Chernyshkov, P.P., Morozov, E.G. and Neiman, V.G., 2004. Structure and Variability of the Falkland Current. *Doklady Earth Sciences*, 399(8), pp. 1156-1159.

14. Franco, B.C., Piola, A.R., Rivas, A.L., Baldoni, A. and Pisoni, J.P., 2008. Multiple Thermal Fronts near the Patagonian Shelf Break. *Geophysical Research Letters*, 35(2), L02607. https://doi.org/10.1029/2007GL032066

15. Piola, A.R., Franco, B.C., Palma, E.D. and Saraceno, M., 2013. Multiple Jets in the Malvinas Current. *Journal of Geophysical Research: Oceans*, 118(4), pp. 2107-2117. https://doi.org/10.1002/jgrc.20170

16. Artana, C.I., Ferrari, R., Koenig, Z., Saraceno, M., Piola, A.R. and Provost, C., 2016. Malvinas Current Variability from Argo Floats and Satellite Altimetry. *Journal of Geophysical Research: Oceans*, 121(7), pp. 4854-4872. https://doi.org/10.1002/2016JC011889

17. Artana, C.I., Lellouche, J.M., Park, Y.H., Garric, G., Koenig, Z., Sennéchael, N., Ferrari, R., Piola, A.R., Saraceno, M. [et al.], 2018. Fronts of the Malvinas Current System: Surface and Subsurface Expressions Revealed by Satellite Altimetry, Argo Floats, and Mercator Operational Model Outputs. *Journal of Geophysical Research: Oceans*, 123(8), pp. 5261-5285. https://doi.org/10.1029/2018JC013887

18. Saraceno, M., Provost, C. and Piola, A.R., 2005. On the Relationship between Satellite-Retrieved Surface Temperature Fronts and Chlorophyll a in the Western South Atlantic. *Journal of Geophysical Research: Oceans*, 110(C11), C11016. https://doi.org/10.1029/2004JC002736

19. Sokolov, S. and Rintoul, S.R., 2007. On the Relationship between Fronts of the Antarctic Circumpolar Current and Surface Chlorophyll Concentrations in the Southern Ocean. *Journal of Geophysical Research: Oceans*, 112(C7), C07030. https://doi.org/10.1029/2006JC004072

20. Chapman, C.C., Lea, M.-A., Meyer, A., Salée, J.-B. and Hindell, M., 2020. Defining Southern Ocean Fronts and Their Influence on Biological and Physical Processes in a Changing Climate. *Nature Climate Change*, 10, pp. 209-219. https://doi.org/10.1038/s41558-020-0705-4

21. Morozov, E.G., Tarakanov, R.Yu., Demidova, T.A., Frey, D.I., Makarenko, N.I., Remeslo, A.V. and Gritsenko, A.M., 2016. Velocity and Transport of the Falkland Current at 46°S. *Russian Journal of Earth Sciences*, 16(6), ES6005. https://doi.org/10.2205/2016ES000588

22. Frey, D.I., Piola, A.R., Krechik, V.A., Fofanov, D.V., Morozov, E.G., Silvestrova, K.P., Tarakanov, R.Yu. and Gladyshev, S.V., 2021. Direct Measurements of the Malvinas Current Velocity Structure. *Journal of Geophysical Research: Oceans*, 126(4), e2020JC016727. https://doi.org/10.1029/2020JC016727

23. Artamonov, Yu.V., 2000. Seasonal Variability of the Position of the Subantarctic Front in the South-West Atlantic Ocean. *Reports of the National Academy of Sciences of Ukraine*, (10), pp. 115-120 (in Russian).

24. Reynolds, R.W., Smith, T.M., Liu, C., Chelton, D.B., Casey, K.S. and Schlax, M.G., 2007. Daily High-Resolution-Blended Analyses for Sea Surface Temperature. *Journal of Climate*, 20(22), pp. 5473-5496. https://doi.org/10.1175/2007JCLI1824.1

25. Matano, R.P., Schlax, M.G. and Chelton, D.B., 1993. Seasonal Variability in the Southwestern Atlantic. *Journal of Geophysical Research: Oceans*, 98(C10), pp. 18027-18035. https://doi.org/10.1029/93JC01602

Submitted 04.03.2024; approved after review 06.05.2024;
accepted for publication 16.05.2024.

About the authors:

Yuri V. Artamonov, Leading Researcher, Marine Hydrophysical Institute of RAS (2 Kapitanskaya Str., Sevastopol, 299011, Russian Federation), DSc. (Geogr.), **ResearcherID: AAC-6651-2020**, **ORCID ID: 0000-0003-2669-7304**, artam-ant@yandex.ru

Elena A. Skripaleva, Chief Researcher, Marine Hydrophysical Institute of RAS (2 Kapitanskaya Str., Sevastopol, 299011, Russian Federation), CSc. (Geogr.), **ResearcherID: AAC-6648-2020**, **ORCID ID: 0000-0003-1012-515X**, sea-ant@yandex.ru

Nikolay V. Nikolsky, Junior Researcher, Marine Hydrophysical Institute of RAS (2 Kapitanskaya Str., Sevastopol, 299011, Russian Federation), **ResearcherID: AAT-7723-2020**, **ORCID ID: 0000-0002-3368-6745**, nikolsky.geo@gmail.com

Contribution of the authors:

Yuri V. Artamonov – general scientific supervision of the research, setting of study aims and objectives, qualitative analysis of the results and interpretation thereof, discussion of the study results, conclusions formulation

Elena A. Skripaleva – review of the literature on the research problem, qualitative analysis of the results and interpretation thereof, processing and description of the study results, discussion of the study results, conclusions formulation, article text preparation

Nikolay V. Nikolsky – development and debugging of computer programs for data processing and carrying out the necessary calculations, computer implementation of algorithms, graphs and diagrams construction, participation in the discussion of article materials

The authors have read and approved the final manuscript.
The authors declare that they have no conflict of interest.